

Nanocups with dynamic metal-nanoparticle inclusion complexes

Mariana Alarcón-Correa,^[a,b] Tung-Chun Lee,^{*,[a,c]} and Peer Fischer^{*,[a,b]}

Abstract: Host-guest inclusion complexes are abundant in molecular systems and of fundamental importance in living organisms. Realizing a colloidal analogue of a molecular dynamic inclusion complex is challenging, because inorganic nanoparticles (NPs) with a well-defined cavity and portal are difficult to synthesize in high yield and with good structural fidelity. Herein, we report a generic strategy towards the fabrication of dynamic 1:1 inclusion complexes of metal nanoparticles inside oxide nanocups with high yield (>70%) and regio-specificity (>90%) by means of a reactive double Janus nanoparticle intermediate. We provide experimental evidence that the inclusion complexes are formed via kinetically controlled mechanism involving a delicate interplay between bipolar galvanic corrosion and alloying-dealloying oxidation. Release of the NP guest from the nanocups can be efficiently triggered by an external stimulus.

Encapsulation underpins a number of fundamental processes in living systems and occurs at multiple length scales, ranging from the inclusion of small molecules within enzymatic pockets to the compartmentalization in cells by lipid bilayers. Artificial encapsulation systems, including bio-inspired ones have been realized with macrocyclic molecules, liposomes, polymerosomes, mesoporous materials,^[1] and metal-organic frameworks (MOFs).^[2] These systems show promise in catalysis and drug delivery.^[3] However, the encapsulation of functional nanomaterials, e.g. metal nanoparticles (NPs), within a well-defined nanoscale cavity remains challenging. While NPs with a concave (negative) curvature, including nanobowls,^[4] concave nanocubes,^[5] and cap-shaped NPs^[6] have been reported, the formation of metal-NP inclusion complexes has so far not been demonstrated.

Herein, we report a generic scheme for the high-yield growth of oxide nanocups and their dynamic 1:1 inclusion complexes with metal NPs selectively located deep inside the cavity (Figure 1). The size of the nanocups lies between that of small viruses, e.g. cowpea mosaic virus, and large enzymes, e.g. F₀F₁-ATP synthase. The nanocups of this Communication encapsulate and can release a ~10-nm gold NP (Au NP). The nanocups can readily be functionalized and their well-defined portal allows small molecules to access the nano-cavity and the nano-confined Au NP, which facilitates the triggered release of

the Au NP. The nanocup could potentially be a means to stabilize the guest NPs in a number of environments, including solvents where the NPs normally cannot be stably dispersed.

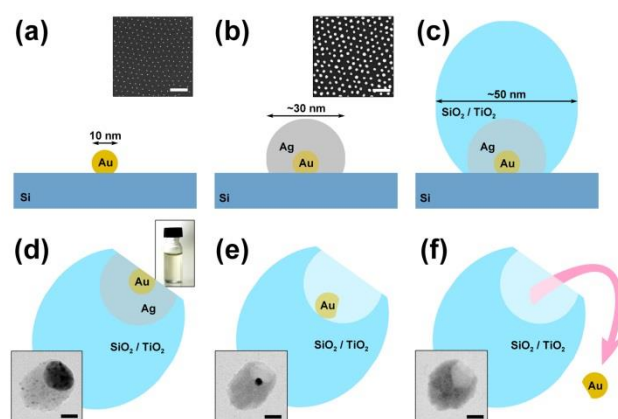


Figure 1. Fabrication scheme of 1:1 Au NP@nanocup inclusion complexes. (a) Quasi-hexagonal pattern of Au NPs made by BCML. (b) Au-Ag Janus NPs grown by Tollens reaction. (a) - (b) inset: SEM images scale bars = 200 nm. (c) Oxide deposition by GLAD, to generate Au-Ag-oxide d-JNPs. (d) Lift off of d-JNPs by sonication. (Top right inset: Photo of the solution). (e) 1:1 inclusion complex obtained upon oxidative dissolution of silver. (f) Release of the Au NP guest triggered by an external stimulus, resulting in empty nanocups. (e) - (f) Inset: TEM images scale bars = 20 nm.

The generation of the inclusion complex of a Au NP inside a nanocup is achieved by a combination of physical vapor deposition and wet chemical processes (Figure 1). First, block-copolymer micelle nanolithography (BCML) is used to pattern a quasi-hexagonal array of monodisperse Au NPs (~10 nm) on a large flat substrate, such as a silicon wafer (Figure 1a).^[7] In a second step, metallic silver is grown on the Au NPs by a Tollens reaction, yielding ~30 nm Au-Ag Janus NPs (JNPs) (see Figure 1b).^[8] The thickness of the silver layer can be controlled by varying the reaction time and the concentration of the reactants. In a subsequent step, an oxide material, such as SiO₂, TiO₂, or Al₂O₃, is deposited on the Ag layer by the physical vapor glancing angle deposition (GLAD) method (Figure 1c).^[9] In essence the wafer is held at a shallow angle with respect to the vapor flux to permit shadow deposition only on the Au-Ag NPs (and not the interstitial space). We have previously shown that the deposited materials smoothly interface with the seeds^[10] and are evenly deposited on the NPs, including the sides. Hence the shape of the seed determines the morphology of the nanocup cavity (see below). Interestingly, after the deposition process, the original seeds, which are themselves Au-Ag JNPs, now become Au-Ag-oxide double Janus NPs (d-JNPs), i.e. JNPs of JNPs. These d-JNPs can then be efficiently removed from the wafer by sonication in aqueous ethanol (Figure 1d). A 1-cm² wafer sample contains ~2.0 × 10¹⁰ NPs which can result in 1 mL of nanocolloidal solution with a concentration comparable to that of commercially available Au nanocolloids of a similar size.^[11] In the final fabrication step, metallic silver is oxidized and dissolved upon the addition of hydrogen peroxide (H₂O₂) in the presence

[a] M. Alarcón-Correa, Dr. T.-C. Lee, Prof. Dr. P. Fischer
Max Planck Institute for Intelligent Systems, Heisenbergstrasse 3,
70569 Stuttgart, Germany
Email: fischer@is.mpg.de

[b] M. Alarcón-Correa, Prof. Dr. P. Fischer
Inst. for Phys. Chem., Univ. Stuttgart, Pfaffenwaldring 55, 70569
Stuttgart, Germany

[c] Dr. T.-C. Lee
Institute for Materials Discovery, University College London,
Kathleen Lonsdale Building, Gower Place, London WC1E 6BT, UK
Email: tungchun.lee@ucl.ac.uk

of aqueous ammonia ($\text{NH}_{3(\text{aq})}$). This results in 1:1 Au NP@nanocup inclusion complexes shown in Figure 1e.

Scanning electron microscopy (SEM) and transmission electron microscopy (TEM) were used to characterize the morphology of the nanostructures. Statistical analysis of 500 NPs reveals that ~70% of the nanocups encapsulate one and only one Au NP. Multiple NP encapsulation is found to be negligible (< 5%), (SI section S4). The cavity dimensions are well controlled, with a standard deviation below 15%, demonstrating a high structural fidelity of our nanocups (Figure 2, and SI section S5). Using angle-dependent TEM we have verified that the Au NP is indeed encapsulated deep inside the nanocup cavity (Figure S2, S9).

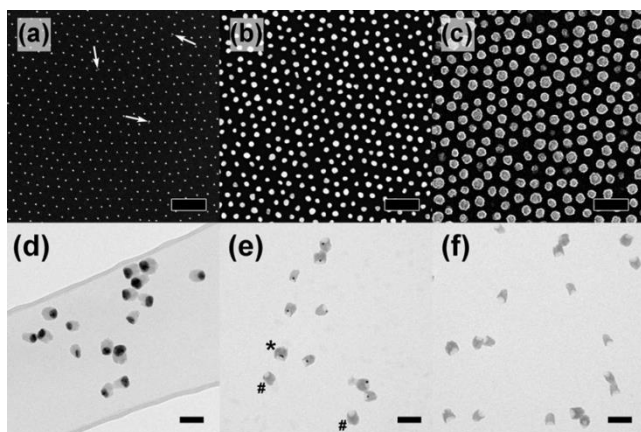


Figure 2. (a) – (c) SEM images of an array of (a) Au NPs (diameter = 8 ± 0.9 nm). Dimeric Au NPs are marked by white arrows; (b) Au-Ag JNPs (diameter = 32.8 ± 4.5 nm); (c) Au-Ag-SiO₂ d-JNPs (diameter = 49.8 ± 9.2 nm). Scale bars = 200 nm. (d) – (f) TEM images of (d) Au-Ag-SiO₂ d-JNPs; (e) Au NP@SiO₂ nanocup inclusion complexes. 2:1 inclusion complex marked by “*” and empty nanocups marked by “#”; (f) Empty SiO₂ nanocups obtained after decomplexation. Scale bars = 100 nm. Formation of 2:1 complexes is believed to be a result of the dimeric Au NP seeds originated in the BCML process.

Scanning TEM energy dispersive X-ray (STEM-edx) and energy-filtered TEM (EF-TEM) analyses were conducted on both the d-JNPs and the inclusion complexes to confirm the designed elemental composition and distribution (Figure 3, S4). Furthermore, to illustrate that our scheme is generic and permits the use of a range of functional materials, we have additionally fabricated 1:1 inclusion complexes of (1) Au NP@TiO₂ nanocups and (2) Au NP@Al₂O₃ nanocups (Figure S5, S6).

The Au NPs do not leave the cups and are almost all (over 90%) located deep inside the nanocup cavity (SI section S6). While there is no material difference between the cavity and the outer surface of the nanocup, the curvature differs. However, this alone is not sufficient to explain, in terms of thermodynamics, the high tendency towards the formation of inclusion complexes plus the unexpectedly high specificity towards the binding ratio and location within the cavity. Hence kinetic factors are very likely to play a crucial role. In order to gain a better understanding of the reaction intermediates, we monitored the silver distribution and the relative position of the Au NP with EF-TEM in samples prepared from a quenched reaction mixture of the oxidation step (Figure 4). The proposed reaction scheme is

as follows: Upon addition of H₂O₂ and NH_{3(aq)} to the d-JNPs, reduction of H₂O₂ preferentially occurs on the cathodic region around the Au NP (red arrow), while bipolar galvanic oxidation of metallic silver is mediated by the electron transfer across the Ag-Au interface (purple arrow), with silver(I) solubilized in the form of [Ag(NH₃)₂]⁺ (green arrow) (Figure 4f). This is similar to the recently reported auto-polarization effects of the Cu-Pt bimetallic micro-swimmers.^[12] In our case, the rate of oxidative dissolution is enhanced at the edge that is farthest away from the Au NP, leading to the formation of a pre-cavity (Figure 4g). Nevertheless, when the solvent-silver interface retreats into the pre-cavity of the nanocup, diffusion of the solvated species around the interface – and hence the bipolar galvanic mechanism – is considerably hindered. At this stage, we suspect that diffusion processes become important, where silver atoms diffuse through the Au NP via alloying or around the Au NP by surface diffusion and are directly oxidized on the gold surface (Figure 4h, red arrow). It has been reported that solid-phase diffusion processes are four to five orders of magnitude more pronounced for nanoparticles, compared to the bulk at room temperature.^[13] The concentration gradient of silver atoms across the Au NP is maintained by the continuous oxidative dissolution of silver on the outer surface of the Au NP. This outward atomic flux of silver results in a net displacement of the Au NP in the opposite direction towards the bottom of the nanocup cavity. Since diffusion of silver in gold is faster than that of gold in silver,^[14] vacancies and voids within the silver will be created (Kirkendall effect) which would then enhance the rate of dissolution of silver via the bipolar galvanic mechanism (positive feedback). After a combination of galvanic and alloying-dealloying corrosion, the Au NP eventually docks at the bottom of the newly formed nanocup cavity and binds with the negatively charged oxide groups formed in an alkaline environment (Figure 4j). This alloying-dealloying mechanism explains why >90% of the Au NPs are found deep inside the cavity. We note that a bipolar galvanic reaction alone would lead to an “immature” release of the Au NP and hence a much lower yield of inclusion complexes plus a random distribution of Au NPs within the cavity.

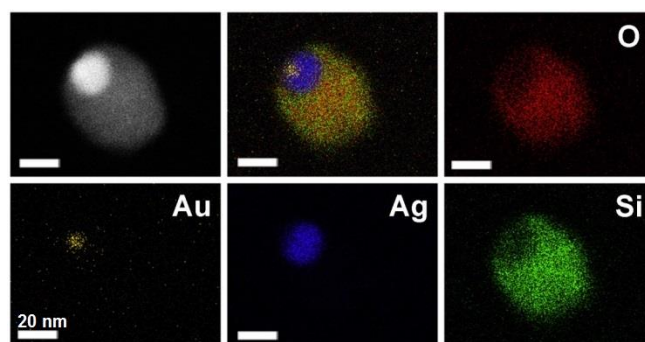


Figure 3. HAADF-STEM image and false-color STEM-edx elemental maps of a Au-Ag-SiO₂ d-JNP. Scale bars = 20 nm. Color codes (and the corresponding transition edges): yellow, gold (Au L); blue, silver (Ag L); green, silicon (Si K); red, oxygen (O K).

It is noted that our system differs from “yolk/shell nanoparticles”^[15] in the way that regio-specific binding and triggered release of the guest NP can only be achieved in our case. Since the Au NP is stabilized in the nanocup by the

negatively charged oxide groups on the SiO₂ surface, the encapsulated Au NP can be efficiently released upon a decrease in pH (causing protonation of the surface oxide groups) or addition of a competitive ligand, such as a water-

soluble thiol, resulting in a solution of free Au NPs and empty oxide nanocups (Figure 1f, 2f. SI Figure S3, S10, S11).

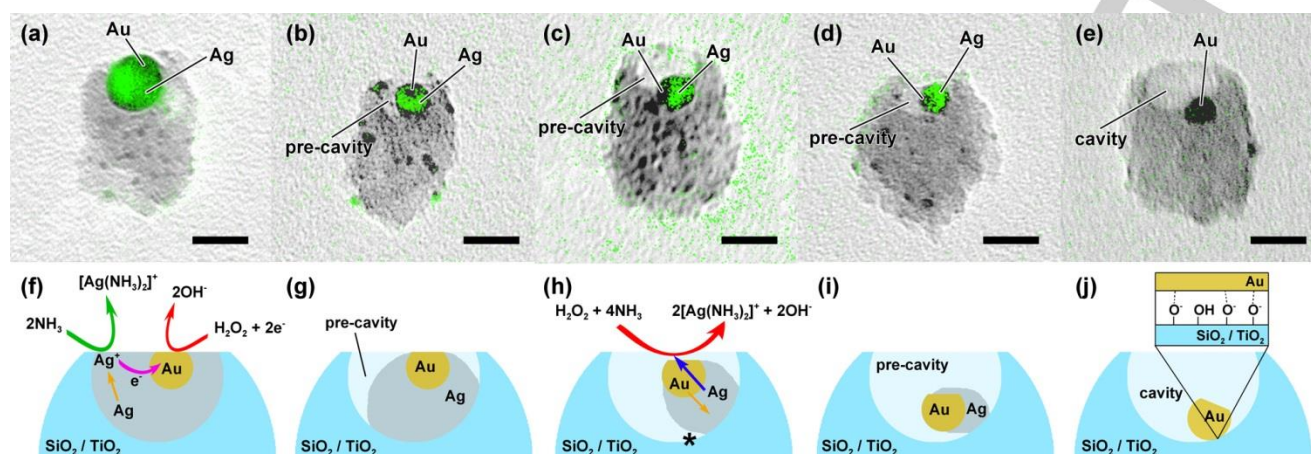


Figure 4. Proposed formation mechanism of the inclusion complexes. Silver distribution maps (green, Ag M_{4,5}) overlaid onto the corresponding bright field TEM images of the (a) Au-Ag-SiO₂ d-JNP, (b) – (d) reaction intermediates, and (e) Au NP@SiO₂ nanocup inclusion complex. Scale bars = 20 nm. (f) – (j) Respective schematic diagrams of the proposed formation mechanism (see main text for details).

In summary, we have realized a nanocolloidal analogue of a “supramolecular host-guest system” consisting of oxide nanocup hosts and their metal nanoparticle guests. A parallel bottom-up growth scheme is used to first fabricate double Janus nanoparticles that are reacted in solution to yield the metal NP@nanocups complexes. A kinetically-controlled bipolar galvanic corrosion and an alloying-dealloying effect results in nanocups of high yield and very high structural fidelity, with a single Au NP located inside the nanocup at a well-defined location. We have also demonstrated the triggered release of the NP guest in response to an external stimulus. To the best of

our knowledge this is the first dynamic metal-NP inclusion complex. Our scheme offers an efficient route to fabricate d-JNPs and metal NPs@ceramic nanocup inclusion complexes. It opens possibilities in stabilizing NPs in solvent environments where the NPs would otherwise not form stable colloidal solutions. This can be achieved without directly functionalizing the metal NPs. The confined geometrical inclusion of the metal NP may in addition open possibilities in the targeted delivery of molecules or reactive NPs. The confined geometry can be used to realize a catalytic nano-reactor with defined structure.

Experimental Section

Materials: Polystyrene (1056)-block-poly (2-vinylpyridine)(495) was supplied by Polymer Source, Canada. Silicon (100) wafers were supplied by CrysTec GmbH, Germany. All chemicals are analytical grade and were used as received unless otherwise stated. Deionized water with 18.2 MΩ resistivity was generated by a Milli-Q ultrapure system.

Preparation of the Au NP array, growth of metallic silver on the Au NP seeds, and the deposition of ceramic materials were conducted based on modified procedures of previous reports, and detailed in the Supporting Information. d-JNPs were lifted off from the wafer by sonicating a sample wafer piece (~1 cm²) in 50% (v/v) aqueous ethanol for ~20 min, resulting in a pure nanocolloidal solution. To 1 mL of this solution, aqueous ammonia (10 μL, 4.0 M), and H₂O₂ (20 μL, 0.8% w/w) were added. After 15 min, the 1:1 inclusion complexes were separated by centrifugation (12100 g, 60 min). The supernatant was removed and the inclusion complexes were re-dispersed in 1 mL of 50% aqueous ethanol by sonication. To release the Au NPs from the nanocups, 25 μL of concentrated HNO₃ (15 M) was added to the solution of inclusion

complexes. After 30 min, the empty nanocups were separated by centrifugation (12100 g, 60 min). The supernatant was removed and the empty nanocups were re-dispersed in 50% aqueous ethanol by sonication.

Acknowledgements

The authors are grateful to C. Miksch and J.P. Spatz for the support on the SEM, BCML and Tollens reaction. We thank the Stuttgart Center for Electron Microscopy for TEM support. We are grateful to A. G. Mark for constructing the 3-D models of the nanostructures, and H.-H. Jeong for helpful comments. This work was in part supported by the European Research Council under the ERC Grant agreement 278213. The authors declare no competing financial interest.

Keywords: Glancing angle deposition • Hybrid nanostructures • Inclusion complexes • Janus nanoparticles • Nanocups

[1] M. Liang, S. Angelos, E. Choi, K. Patel, J. F. Stoddart, J. I. Zink, *J. Mater. Chem.* **2009**, *19*, 6251–6257.

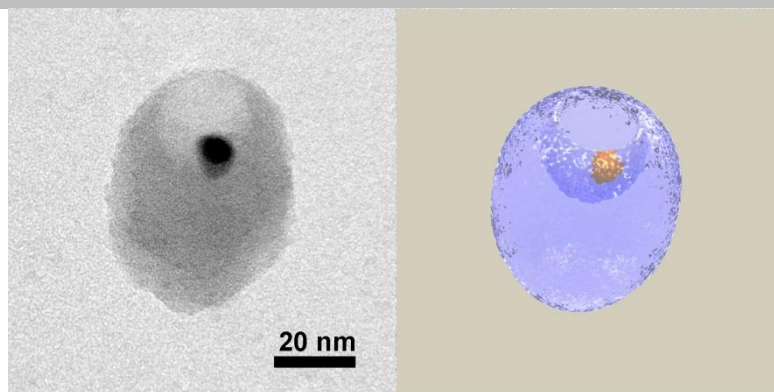
- [2] M. Kiguchi, J. Inatomi, Y. Takahashi, R. Tanaka, T. Osuga, T. Murase, M. Fujita, T. Tada, S. Watanabe, *Angew. Chem. Int. Ed.* **2013**, *52*, 6202–6205; *Angew. Chem.* **2013**, *125*, 6322–6325.
- [3] a) F. Hof, S. L. Craig, C. Nuckolls, J. Rebek, Jr., *Angew. Chem. Int. Ed.* **2002**, *41*, 1488–1508; *Angew. Chem.* **2002**, *114*, 1556–1578; b) X. J. Loh, J. del Barrio, P. P. C. Toh, T.-C. Lee, D. Jiao, U. Rauwald, E. A. Appel, O. A. Scherman, *Biomacromolecules* **2012**, *13*, 84–91; c) D. Jiao, J. Geng, X. J. Loh, D. Das, T.-C. Lee, O. A. Scherman, *Angew. Chem. Int. Ed.* **2012**, *51*, 9633–9637; *Angew. Chem.* **2012**, *124*, 9771–9775.
- [4] Y. Ridelman, G. Singh, R. Popovitz-Biro, S. G. Wolf, S. Das, R. Klajn, *Small* **2012**, *8*, 654–660.
- [5] a) J. A. Zhang, M. R. Langille, M. L. Personick, K. Zhang, S. Y. Li, C. A. Mirkin, *J. Am. Chem. Soc.* **2010**, *132*, 14012–14014; b) T. Yu, D. Y. Kim, H. Zhang, Y. Xia, *Angew. Chem. Int. Ed.* **2011**, *50*, 2773–2777; *Angew. Chem.* **2011**, *123*, 2825–2829.
- [6] a) Y. M. Lee, M. A. Garcia, N. A. F. Huls, S. H. Sun, *Angew. Chem. Int. Ed.* **2010**, *49*, 1271–1274; *Angew. Chem.* **2010**, *122*, 1293–1296 b) N. N. Zhao, L. S. Li, T. Huang, L. M. Qi, *Nanoscale* **2010**, *2*, 2418–2423.
- [7] R. Glass, M. Möller, J. P. Spatz, *Nanotechnology* **2003**, *14*, 1153–1160.
- [8] S. Kruss, V. Srot, P. A. van Aken, J. P. Spatz, *Langmuir* **2012**, *28*, 1562–1568.
- [9] M. M. Hawkeye, M. J. Brett, *J. Vac. Sci. Technol. A* **2007**, *25*, 1317–1335.
- [10] A. G. Mark, J. G. Gibbs, T.-C. Lee, P. Fischer, *Nat. Mater.* **2013**, *12*, 802–807.
- [11] <http://www.sigmaaldrich.com/catalog/product/aldrich/742015?lang=de®ion=DE>
- [12] R. Liu, A. Sen, *J. Am. Chem. Soc.* **2011**, *133*, 20064–20067.
- [13] E. González, J. Arbiol, V. F. Puentes, *Science* **2011**, *334*, 1377–1380.
- [14] Y. Sun, Y. Xia, *J. Am. Chem. Soc.* **2004**, *126*, 3892–3901.
- [15] J. Liu, S. Z. Qiao, J. S. Chen, X. W. (D.) Lou, X. Xing, G. Q. (M.) Lu, *Chem. Commun.* **2011**, *47*, 12578–12591.

Entry for the Table of Contents (Please choose one layout)

Layout 1:

COMMUNICATION

Nanocups with a Au NP: Dynamic inorganic host-guest nanostructure with a metal nanoparticle (guest) located deep inside an oxide nanocup (host).



Mariana Alarcón-Correa,^[a,b] Tung-Chun Lee,^{ [a,c]} and Peer Fischer^{* [a,b]}*

Page No. – Page No.

Nanocups with dynamic metal-nanoparticle inclusion complexes